Graphene field effect transistor for ultrasensitive label-free detection of ATP and Adenosine

Jianjian Liu*, *Meng* Tian, *Ruihong* Song, *Yingxian* Li, *Zanxia* Cao, *Qiang* Li, *Jian* Liu, *Shicai* Xu, *Jihua* Wang

Dezhou University, Institute of Biophysics, Shandong Engineering Laboratory of Swine Health Big Data and Intelligent Monitoring, Shandong Key Laboratory of Biophysics, Dezhou, China

Abstract. Because of unique electrical and structural properties, graphene has attracted widespread attention in biosensing applications. In this paper, a single layer of graphene was grown by chemical vapor deposition (CVD). Using graphene as the electric channel, a graphene field effect transistor (G-FET) biosensor was fabricated and used to detect adenosine triphosphate (ATP) and adenosine. Compared with traditional methods, the G-FET biosensor has the advantages of higher sensitivity and better stability. The sensor showed high performance and achieved a detection limit down to 0.5 pM for both ATP and adenosine. Moreover, the G-FET biosensor showed an excellent linear electrical response to ATP concentrations in a broad range from 0.5 pM to 50 μM. The developed graphene biosensor has high sensitivity, simple operation, and fast analysis speed, which may provide a new feasible direction to detect ATP and adenosine. Healthy sexually mature male laboratory Wistar rats, weighing 180-200 gr ("FSUE "Nursery of laboratory animals "Rappolovo") and having been placed under quarantine not less than for 14 days, were selected for the experiment.

1 Introduction

In the past few decades, a great deal of research in new sensing technologies/sensors has focused on surface enhanced Raman spectroscopy (SERS) [1], electrochemistry [2, 3], capacitor sensor, and surface plasmon resonance (SPR) [4, 5]. These sensors have been widely used for chemical and biomolecule detection, but they are difficult to operate at low cost and be miniaturized for measurement [6]. Compared with these sensors, the field effect transistor (FET) electronic sensor has been confirmed to have tremendous potential to detect many kinds of analytes due to its high sensitivity, fast detection speed, low cost and simple operation [7-11].

Graphene is a kind of nanomaterial consisting of one single layer of carbon atoms arranged in a two-dimensional (2D) hexagonal crystal [12]. Graphene has many remarkable physical properties due to its unique 2D structure, such as massless carriers (electrons and holes), high transparency (97.7% for single layer), high conductivity, large specific surface area (2630 $m^2 \bullet g^{-1}$), and high carrier mobility (up to 105 $cm \bullet V^{-1} \bullet s^{-1}$), which is about 2-3 orders of magnitude higher than typical semiconductors like silicon [13-15]. Therefore, FET biosensors prepared using graphene have been extensively studied, and these sensors have been confirmed to have tremendous potential to detect many kinds of analyses [16-18]. Xu *et al.* developed a multi-channel graphene biosensor for real-time reliable determination of binding kinetics of DNA hybridization [6]. Zhang *et al.* built a sensor platform using graphene and metal oxide nanoparticles (NPs) for high selective and fast responsive hydrogen gas detection [19]. Wang *et al.* presented an affinity graphene nanosensor for detecting biomarkers in undiluted and non-desalted human serum [20]. Compared with 1D nanomaterials such as silicon nanowires [21, 22] and carbon nanotubes[23, 24], graphene has a high surface-tovolume ratio and can intimately contact with metal electrodes because of their large surface area. Therefore, it is easier to manipulate and control the channel structure in the graphene field effect transistor (G-FET) sensor, showing great advantages in manufacturing and wide applications [25-29]. In this study, we developed a G-FET biosensor to detect adenosine and adenosine triphosphate (ATP). Adenosine is an endogenous nucleoside distributed throughout the cells and can be directly phosphorylated to form adenylate. It is an endogenous anticonvulsant and an epileptic terminator [30, 31]. Adenosine signaling also plays an important role in regulating tumor immunity [32]. Adenosine triphosphate (ATP) is a multi-function chemical signaling agent that is the main energy molecule of the cells and plays a critical role in signal transduction in organisms. The fluctuation of ATP concentration is closely related to many diseases such as suppuration, hypoglycemia, and some malignant tumors [33, 34]. In addition, ATP has a wide range of applications in environmental monitoring [35, 36], drug analysis [37], food safety [38], *etc*. To date, many detection methods of adenosine and ATP have been previously proposed, including colorimetry [39, 40], liquid chromatography [41, 42], fluorescence analysis [43, 44],

* Corresponding author: ljianjian1994@163.com

chemiluminescence [45], electrochemical methods [46, 47], *etc*. However, these methods still suffer from complex experimental operations, difficulties in preparing the reagents used, and needs for expensive instruments.

In this work, we developed a field effect transistor (GFET) biosensor using graphene as an electron channel for adenosine and ATP detection. The LOD of the G-FET sensor is as low as 0.5 pM. Compared with traditional adenosine and ATP detection methods, the G-FET sensor has high sensitivity, fast analysis speed, simple operation, and low cost. This biosensor may provide a new approach for the detection of adenosine and ATP.

2 Experimental

Materials and reagent. Glass substrates of indium tin oxide (ITO) conductive film were purchased from South China Xiangcheng (Shenzhen, China) Co., Ltd. ATP, adenosine and PMMA were purchased from Aladdin Industrial Corporation. Ag/AgCl electrodes were purchased from Yancheng Arduino Analytical Instruments (Jiangsu) Co., Ltd. The Cu foil (purity: 99.99 %, thickness: 50 μm) was purchased from Afaisha. (Tianjin, China). The $FeCl_3$ was purchased from Shanghai Aibi Chemical Reagent Co., Ltd.

Preparation of graphene. The copper foil was first ultrasonic cleaned with ethanol and deionized water for 20 minutes. After drying with nitrogen, the copper foil was placed in the tube furnace, and graphene film was grown on the copper substrate by chemical vapor deposition (CVD) at 1050 ℃. First, the copper foil was annealed at 1050 °C for 10 minutes with a hydrogen flow of 30 sccm to improve the quality of graphene. Then, the gas mixture of methane (10 sccm) and hydrogen (30 sccm) was introduced into quartz tube for 10 min to grow graphene. Finally, the samples were rapidly cooled to room temperature with a hydrogen flow of 30 sccm.

Fabrication of G-FETs. We obtained the graphene grown on copper by wet transfer. First, polymethyl methacrylate (PMMA) was used as the protective layer to transfer the as-grown graphene films [48]. The graphene/Cu foil was spin-coated with PMMA acetone solution at low speed for 5 seconds (500 rpm) and at high speed for 30 seconds (4000 rpm) in sequence to make PMMA uniformly dispersed on the surface of the graphene. Then, the samples were baked at 150 ℃ for 30 minutes to make the PMMA layer closely adhered to the graphene. After cooling to room temperature, the PMMA/graphene/Cu was placed in $FeCl_3$ solution to etch the copper foil. Then, we put the PMMA/graphene in deionized water to remove residual $FeCl_3$. The obtained PMMA/graphene film was transferred onto the glass substrate, where the ITO was used as the source electrode and the drain electrode. Then, the PMMA/graphene/substrate was placed on a hot plate at 180 ℃ for 30 minutes to remove moisture and to make graphene adhered to the substrate. After that, the PMMA/graphene/substrate was immersed in an acetone solution for 24 hours to remove PMMA, thereby leaving graphene as an electric channel between the substrate source electrode and the drain electrode. Finally, a sample cell (φ = 0.5 mm) was mounted on the graphene to add adenosine and ATP for detection. An Ag/AgCl electrode was inserted as a reference electrode into the sample cell to provide a gate voltage (Vgs).

Detection of ATP and Adenosine. We obtained the standard ATP and adenosine solution by adding 5.1 mg of ATP and 2.7 mg of adenosine separately to 2 ml of deionized water. Then, the standard solution was diluted to get a series of ATP and adenosine samples with different concentrations for detection. For measurements of transfer characteristics (drain current vs. gate voltage) of the GFETs, the drain voltage (Vds) was set to 10 mV. The gate voltage (Vgs) varied with a sweeping step of 10 mV, and for each step, the given Vgs pulse was maintained for 1 s to stabilize drain current (Ids) to ensure the reliability of the transfer curve.

Characterization and electronic measurement. The morphology of the graphene was characterized by scanning electron microscopy (SEM ZEISS, SUPRATM55). The Raman spectrum of the graphene was measured using a Raman spectrometer (Horiba HR-800) with an excitation wavelength of 532 nm and a laser spot of about 0.1 μm. The electrical measurements were performed by a semiconductor parameter analyzer (PDA FS360) coupled with a probe station (PEH-4).

3 Results and discussion

Graphene structure. Graphene film with a large area of 150 mm × 100 mm was fabricated on the copper foil. The large graphene film was cut into lots of pieces with a size of 9 mm × 9 mm × 50 μm for G-FET fabrication. The SEM image of the graphene grown on the copper foil is shown in Fig. 1a. A few light ridges were observed on the surface of the sample. The ridges are expected to be formed during the cooling process, due to the difference of thermal expansion coefficient between graphene and copper [49]. Fig. 1b shows the SEM image of the graphene film transferred onto the glass substrate. The graphene surface on the glass substrate is very flat and continuously without tears and loopholes, indicating that the graphene was well transferred. Fig. 1c shows a typical Raman spectrum collected from the graphene film. The characteristic bands of graphene D (at ~1338 cm^{-1}), G (~1577 cm^{-1}), and 2D (~2681 cm^{-1}) were all observed in this image. The G band is due to the first-order scattering of the in-plane optical phonon *E*2g mode. The 2D band is regarded as characteristic bands of the graphene structure caused by a second-order process involving two photons with opposite momentum [50]. The D band is related to the structural defects, and it is due to the sp2 atoms out-ofplane breathing mode. In most regions of the graphene film, Raman spectroscopy shows typical characteristics of single-layer graphene with an intensity ratio I2D / IG ≥ 2 and a full width at half maximum (FWHM) of about 53 cm^{-1}, indicating that the grown graphene is monolayer

[51]. In addition, the D-bands associated with defects are very weak, indicating the overall high quality of graphene [52]. Fig. 1d shows the optical image of the typical graphene transferred on the SiO_2/Si substrates. In the optical micrograph of the graphene film, different shades of color reflect different thicknesses of graphene. In our case, the uniform color contrast of the optical micrograph indicates that the film has excellent thickness uniformity.

G-FET drain-source electric current response induced by adenosine. Using the G-FET sensor, we detected the adenosine in a wide concentration range from 0.5 pM to 50 μM (Fig. 2). Fig. 2 shows the typical transfer characteristics of the G-FET sensor to detect adenosine with different concentrations. Here, the typical ambipolar field effect characteristic of graphene was not observed, which can be explained by the doping effects from the substrate or residue produced during the graphene transfer process [53]. In the range from -0.1 to 1.4 V, the transfer curve was almost completely overlapped, show a negligible electrical response to the change of adenosine concentration. When the gate voltage was higher than 1.4 V, the electric current value increases monotonically with increasing Vg, indicating typical n-type behavior.

In the n-type region, the G-FET sensor showed a sensitive electrical response to adenosine concentration. From the transfer curve, the adenosine with different concentrations can be easily distinguished. For a fixed voltage value, the electric current varies with the concentration of the adenosine solution. Especially when the adenosine concentration was lower than 1 nM, the electric current drops sharply, showing extremely high detection sensitivity. The electric current characteristics of 0.5 pM adenosine can be easily distinguished from the blank sample, indicating that the detection of limit (LOD) was even lower than 0.5 pM. The high sensitivity of the G-FET sensor can be attributed to the high surface-to-volume ratio and high electron mobility of graphene.

G-FET drain-source electric current response induced by ATP. We also detected the ATP in a wide concentration range from 0.5 pM to 50 μM by using the G-FET sensor (Fig. 3). The figure shows the typical transfer characteristics of the G-FET sensor to detect ATP with different concentrations. As similar to adenosine detection, the electric current value increases monotonically with increasing Vgs, indicating typical n-type behavior. In the n-type region, when the gate voltage was higher than 1.4 V, the G-FET sensor showed a sensitive electric current response to ATP concentration. After amplifying the sensor diagram with the sweeping voltage from 1.70 to 1.85 V, it can be clearly seen that the transfer curves of GFET for different ATP concentrations can be well distinguished. The figure also shows the device electric current versus the logarithm of ATP concentration at a certain gate voltage Vgs = 1.70 V and Vgs = 1.85, respectively. For both cases, the electric current decreases linearly as the ATP concentration increases with a good linear correlation in a broad range from 0.5 pM to 50 μM, indicating that the G-FET has the high potential for quantitative detection of ATP.

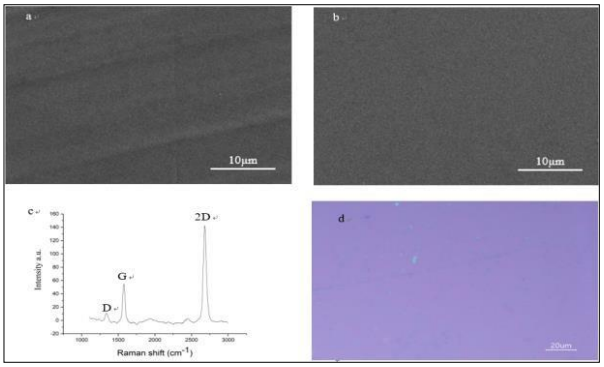

Fig. 1. a: SEM image of the graphene grown on copper foil, b: SEM image of the graphene transferred onto the glass substrate, c: Typical Raman spectrum of the graphene film, d: Optical microscope image of the transferred graphene film on the SiO_2/Si substrate.

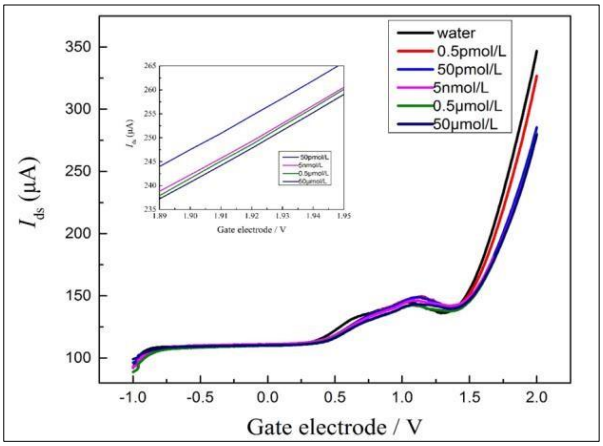

Fig. 2. Typical transfer characteristics of the G-FET sensor for adenosine detection with different concentration with the sweep gate voltage from -1.0 to 2.0, 1.5 to 1.95 V, 1.90 to 1.95 V.

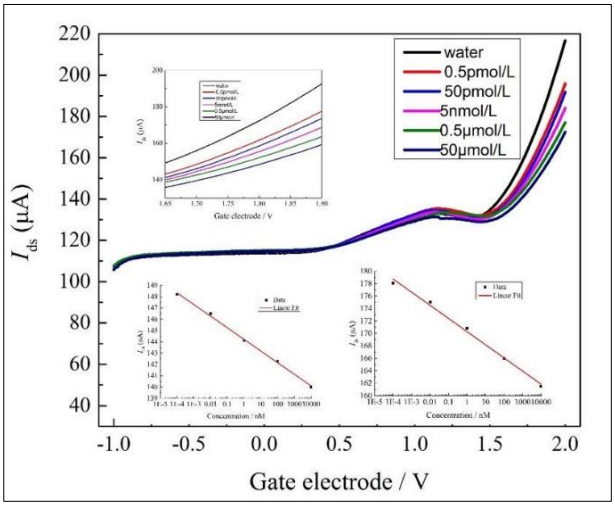

Fig. 3. Typical transfer characteristics of the G-FET sensor for ATP detection with different concentration with the sweep gate voltage from -1.0 to 2.0 V, 1.65 to 1.90 V. Device electric current versus the logarithm of ATP concentration at a certain gate voltage Vgs = 1.70 V and Vgs = 1.85 V.

4 Conclusion

In this work, we developed a G-FET biosensor using graphene as the conductive channel for adenosine and ATP detection. The G-FET biosensor shows high detection sensitivity, and the LOD of the G-FET sensors for both adenosine and ATP is as low as 0.5 pM. The high sensitivity of the G-FET sensor can be attributed to the high surface-to-volume ratio and high electron mobility of graphene. For adenosine detection, the sensor shows extremely high sensitive electrical response, especially when the adenosine concentration was lower than 1 nM. For ATP detection, the G-FET biosensor shows a good linear electric current response to ATP concentrations in a broad range from 0.5 pM to 50 μM, indicating the high potential for quantitative detection of ATP. The G-FET biosensor is label-free and has a low operating voltage and high measurement accuracy, providing a very promising future in the detection of important biomolecules.

5 Acknowledgment

We are grateful for financial support from National Natural Science Foundation of China (11604040, 11674199), and Taishan Scholars Program of Shandong Province (tsqn201812104, tshw201502045), Qing chuang Science and Technology Plan of Shandong Province (2019KJJ017, 2020KJC004), Youth Innovation Team Lead-education Project of Shandong Educational Committee.

6 References

1. P. R. Stoddart and D. J. White, Anal Bioanal Chem, **394**, 1761-1774, (2009)
2. E. Paleček and F. Jelen, Critical Reviews in Analytical Chemistry, **32**, 261-270, (2002)
3. Y. Shao, J. Wang, H. Wu, *et al*., Graphene Based Electrochemical Sensors and Biosensors: A Review Electroanalysis, **22**, 1027-1036, (2010)
4. J. Homola, Anal Bioanal Chem, **377**, 528-539, (2003)
5. S. Qian, Y. Zhang, H. Yuan, *et al*., Sensors and Actuators B: Chemical, **260**, 976-982, (2018)
6. S. Xu, J. Zhan, B. Man, *et al*., Nat Commun, **8**, 14902, (2017)
7. C. M. Hangarter, M. Bangar, A. Mulchandani, *et al*., Journal of Materials Chemistry, **20**, 3131, (2010)
8. Z. Fan, D. Wang, P.-C. Chang, *et al*., Applied Physics Letters, **85**, 5923-5925, (2004)
9. W. Shi, J. Yu and H. E. Katz, Sensors and Actuators B: Chemical, **254**, 940-948, (2018)
10. Y. Chen, R. Ren, H. Pu, *et al*., Biosens Bioelectron, **89**, 505-510, (2017)
11. M. Tian, S. Xu, J. Zhang, *et al*., Advances in Condensed Matter Physics, **2018**, 1-6, (2018)
12. K. S. Novoselov, A. K. Geim, S. V. Morozov, *et al*., Nature, **438**, 197-200, (2005)
13. X. Du, I. Skachko, A. Barker, *et al*., Nat Nanotechnol, **3**, 491-495, (2008)
14. Y. Wu, Y.-m. Lin, A. A. Bol, *et al*., Nature, **472**, 7478, (2011)
15. L. Gao, W. Ren, H. Xu, *et al*., Nature Communications, **3**, (2012)
16. S. Cheng, S. Hideshima, S. Kuroiwa, *et al*., Sensors and Actuators B: Chemical, **212**, 329-334, (2015)
17. X. Liu, P. Lin, X. Yan, *et al*., Sensors and Actuators B: Chemical, **176**, 22-27, (2013)
18. X. Zong and R. Zhu, Sensors and Actuators B: Chemical, **255**, 2448-2453, (2018)
19. Z. Zhang, X. Zou, L. Xu, *et al*., Nanoscale, **7**, 10078-10084, (2015)
20. X. Wang, Y. Zhu, T. R. Olsen, *et al*., Electrochimica Acta, **290**, 356-363, (2018)
21. S. Zafar, M. Khater, V. Jain, *et al*., Applied Physics Letters, **106**, 063701, (2015)
22. Y. Guerfi and G. Larrieu, Nanoscale Res Lett, **11**, 210, (2016)
23. S. Okuda, S. Okamoto, Y. Ohno, *et al*., The Journal of Physical Chemistry C, **116**, 19490-19495, (2012)
24. S. Z. Bisri, V. Derenskyi, W. Gomulya, *et al*., Advanced Electronic Materials, **2**, 1500222, (2016)
25. K. Maehashi, Y. Sofue, S. Okamoto, *et al*., Sensors and Actuators B: Chemical, **187**, 45-49, (2013)
26. P. T. K. Loan, D. Wu, C. Ye, *et al*., Biosens Bioelectron, **99**, 85-91, (2018)
27. Y. M. Lei, M. M. Xiao, Y. T. Li, *et al*., Biosens Bioelectron, **91**, 1-7, (2017)
28. C. Andronescu and W. Schuhmann, Current Opinion in Electrochemistry, **3**, 11-17, (2017)
29. S. Szunerits and R. Boukherroub, Interface Focus, **8**, 20160132, (2018)
30. L. Weltha, J. Reemmer and D. Boison, The role of adenosine in epilepsy, Brain Res Bull, (2018)
31. G. Hasko, L. Antonioli and B. N. Cronstein, Biochem Pharmacol, **151**, 307-313, (2018)
32. R. D. Leone and L. A. Emens, J Immunother Cancer, **6**, 57, (2018)
33. S. L. Zhang, X. Hu, W. Zhang, *et al*., J Med Chem, **59**, 3562-3568, (2016)
34. P. de Andrade Mello, R. Coutinho-Silva and L. E. B. Savio, Front Immunol, **8**, 1526, (2017)
35. G. S. Whiteley, C. Derry, T. Glasbey, *et al*., Infect Control Hosp Epidemiol, **36**, 658-663, (2015)
36. B. D. Lewis, M. Spencer, P. J. Rossi, *et al*., Am J Infect Control, **43**, 283-285, (2015)
37. M. Zhang, N. Zhou, P. Yuan, *et al*., RSC Advances, **7**, 9284-9293, (2017)
38. Z. Zhang, C. Wang, L. Zhang, *et al*., Analytical Methods, **9**, 53785387, (2017)
39. Y. Mao, T. Fan, R. Gysbers, *et al*., Talanta, **168**, 279285, (2017)

40. N. An, Q. Zhang, J. Wang, *et al*., Polymer Chemistry, **8**, 1138-1145, (2017)
41. L. Wagmann, H. H. Maurer and M. R. Meyer, J Chromatogr A, **1521**, 123-130, (2017)
42. J. Domníguez-Álvarez, M. Mateos-Vivas, E. Rodrgíuez-Gonzalo, *et al*., TrAC Trends in Analytical Chemistry, **92**, 1231, (2017)
43. X. M. Hai, N. Li, K. Wang, *et al*., Anal Chim Acta, **998**, 6066, (2018)
44. Q. Zhao, Q. Lv and H. Wang, Biosens Bioelectron, **70**, 188-193, (2015)
45. L.-Y. Yao, X.-Q. Yu, R.-J. Yu, *et al*., Sensors and Actuators B: Chemical, **238**, 175-181, (2017)
46. X. Ding, Y. Wang, W. Cheng, *et al*., Microchimica Acta, **184**,. 431-438, (2016)
47. X. Zhang, C. Song, K. Yang, *et al*., Anal Chem, **90**, 4968-4971, (2018)
48. W. Yue, S. Jiang, S. Xu, *et al*., Sensors and Actuators B: Chemical, **195**, 467-472, (2014)
49. X. Li, W. Cai, J. An, *et al*., Science, **324**, 1312-1314, (2009)
50. V. T. Nguyen, H. D. Le, V. C. Nguyen, *et al*., Advances in Natural Sciences: Nanoscience and Nanotechnology, **4**, 035012, (2013)
51. A. N. Obraztsov, E. A. Obraztsova, A. V. Tyurnina, *et al*., Carbon, **45**, 2017-2021, (2007)
52. Z. Sun, Z. Yan, J. Yao, *et al*., "Growth of graphene from solid carbon sources", Nature, 468, 549-552, 2010.
53. J. Chen, Y. Wen, Y. Guo, *et al*., J Am Chem Soc, **133**, 17548-17551, (2011